



Article

Magnetorheological Hybrid Elastomers Based on Silicone Rubber and Magnetorheological Suspensions with Graphene Nanoparticles: Effects of the Magnetic Field on the Relative Dielectric Permittivity and Electric Conductivity

Ioan Bica and Octavian Mădălin Bunoiu *

Department of Physics, West University of Timisoara, 300223 Timisoara, Romania

* Correspondence: madalin.bunoiu@e-uvv.ro; Tel.: +40-256-592-166

Received: 4 July 2019; Accepted: 24 August 2019; Published: 27 August 2019



Abstract: Hybrid magnetorheological elastomers (hMREs) were manufactured based on silicone rubber, silicone oil, carbonyl iron microparticles, graphene nanoparticles and cotton fabric. Using the hMREs, flat capacitors (FCs) were made. Using the installation described in this paper, the electrical capacitance and the coefficient of dielectric losses of the hMREs were measured as a function of the intensity of the magnetic field superimposed over an alternating electric field. From the data obtained, the electrical conductivity, the relative dielectric permittivity and magnetodielectric effects are determined. It is observed that the obtained quantities are significantly influenced by the intensity of the magnetic field and the amount of graphene used.

Keywords: magnetodielectric effect; hybrid magnetorheological elastomer; membrane; silicone rubber; graphene nanoparticles; carbonyl iron

1. Introduction

Magnetorheological materials consist of a silicone oil-based matrix, mineral oil, elastomer, etc., in which a magnetisable phase and additives are dispersed. The magnetisable phase is in the form of ferro-ferrimagnetic particles, and the additives are in the form of nano-microparticles. The latter can be either electroconductive or dielectric.

In the literature, these materials are known by the generic name “smart materials” [1–8]. They have a certain peculiarity, which consists in the fact that their physical properties change significantly when applying external factors in the form of magnetic fields, electromagnetic fields, mechanical tensions, etc. [9–13]. This property of magnetorheological materials is used in technical applications [14,15]. Recently, due to the increased scientific and applied interest, the scientific community has attributed great importance to magnetorheological elastomers (MREs). In MREs, the magnetisable microparticles and additives are “frozen” by polymerization into the polymer. In this way, the sedimentation coefficient is much lower than that of the magnetorheological suspensions, giving them stable physical properties over time. In a magnetic field, the magnetisable phase in the elastic matrix of the MREs is oriented along the field lines. Aggregates are created in the form of chains, which have the effect of drastically modifying the rheological properties. These properties are of use in the production of vibration and seismic shock dampers [16], and in the development of sensors for mechanical deformation and stresses [17], actuators [18], etc. In Refs. [19–21], it is reported that the electrical conductivity of MREs increases in a magnetic field, which is a useful property in the realization of sensors and actuators [7,9,10].

Recently, academia has been concerned with the study of magnetodielectric materials induced by a magnetic field superimposed on a low-, high- or very high-frequency alternative electric field.

In Ref. [22], the effects induced by magnetic fields in ceramics in a high-frequency electric field are reported. In these materials, the components of the complex dielectric permittivity are noticeably modified in a static magnetic field superimposed over a high frequency electric field. In Refs. [23,24], using magnetic fluids based on Fe nanoparticles, an increase of up to 15% in the magnetodielectric effects was reported through applying a static magnetic field superimposed on an electric field with frequencies of up to 5 MHz. Spectacular increases in magnetodielectric effects were obtained in Ref. [25]. Here, the magnetodielectric effects induced in MREs based on Fe, NdFeB, and Fe₃O₄ microparticles were up to 150% higher when superimposing the static magnetic field over a high-frequency electric field. In a recent paper [26], it was reported that magnetodielectric effects are also relevant in magnetorheological biosuspensions. Here, it was mentioned that magnetodielectric effects can be used for biomedical purposes. This assessment was based on the use of thermal transport of bioactive compounds. Following this research direction, in this paper, hybrid MREs are manufactured. They have in their composition a textile fabric, impregnated with a mixture made of silicone rubber, silicone oil, graphene nanoparticles and carbonyl iron microparticles, which polymerize between two conductive plates. Using the installation described in the paper, measurements of electric capacitance and of coefficients of dielectric losses are made in an alternative electric field with a frequency of 1 kHz, superimposed over a static magnetic one. From the obtained data, the relative dielectric permittivity and electrical conductivity of hMREs are determined. It is shown that the determined quantities depend on the intensity of the external magnetic field and on the composition of the hMREs.

2. Results and Discussion

The experimental setup used to measure the capacitance C and the dielectric loss coefficient D is described in Figure 1. Using the adjustment device, the distances between A and FC are fixed in such a way that the intensity of the magnetic field is increased in steps of 50 kA/m up to values of 250 kA/m. Using the bridge B, we measured the capacitance C and the dielectric loss coefficient D of the FCs in the electric field with $f = 1$ kHz frequency at intervals of $t = 5$ s, starting with the application of the magnetic field. The obtained results are presented in Figure 2.

It can be seen from Figure 2 that the capacitance C and the coefficient of dielectric losses D of the FCs increase with the increase of the intensity H of the external magnetic field. In contrast, for fixed values of H , C and D increase with increasing mass fraction of graphene nanoparticles.

It is known [1–29] that in a magnetic field, the CI microparticles of the hMRE instantaneously become magnetic dipoles. They orient themselves, in time, along the filed lines of the magnetic field. The measurements are performed at fixed intervals of time, and therefore the time-dependence of the measured quantities is not shown in Figure 2.

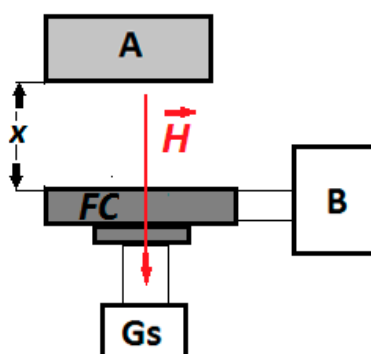


Figure 1. Experimental setup (overall configuration): A—neodymium magnet; B—impedance meter (type ET-20); FC—working flat capacitor; \vec{H} —magnetic field strength vector; Gs—Gaussmeter, type DX-102; h—Hall probe; x —adjustable distance.

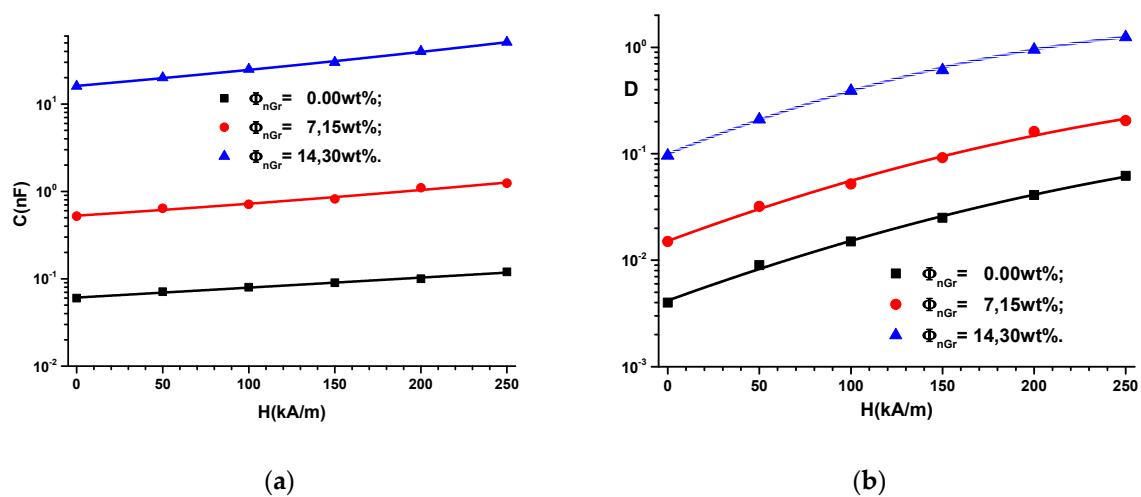


Figure 2. (a) The capacitance C of the FC; (b) the dielectric loss factor D dependence on the intensity H of the magnetic field and on the mass fractions Φ_{nGr} of the graphene nanoparticles.

The capacitance of the FC, neglecting edge effects, can be calculated by:

$$C = \frac{\epsilon_0 \epsilon' L l}{d} \tag{1}$$

where ϵ_0 is the dielectric permittivity of vacuum, ϵ' is the relative dielectric permittivity, L is the length, l is the width and d is the thickness of the membrane.

For $\epsilon_0 = 8.85 \times 10^{-12} \frac{F}{m}$, $L = 50$ mm, $l = 40$ mm and $d = 1.2$ mm, in Expression (1), the relative dielectric permittivity can be obtained as follows:

$$\epsilon' = 67.56 \times C(H)_{\Phi_{nGr}} \tag{2}$$

The functions $C(H)_{\Phi_{nGr}}$ from Figure 2a are inserted in Expression (2), and in Figure 3a, the variation of ϵ' with intensity H of the static magnetic field superimposed on the alternative electric field is obtained.

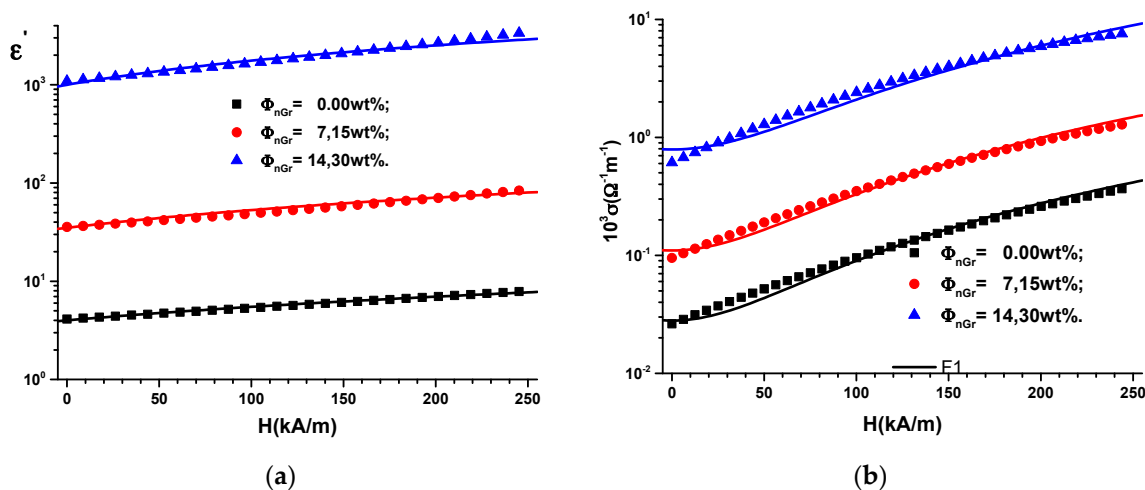


Figure 3. (a) Relative dielectric permittivity ϵ' ; (b) electrical conductivity σ as function of intensity H of the magnetic field and mass fractions Φ_{nGr} of graphene nanoparticles (dots = experimental data, lines = theoretical result).

Due to interfacial polarization of the nanographene [30], the relative dielectric permittivity of the nMRE (Figure 3a) increases with H and is noticeably influenced by the increase in nanographene mass

fraction Φ_{nGr} . Variation of the relative dielectric permittivity ε' with the intensity H of the magnetic field for the used quantities of graphene can be approximated, as can be observed in Figure 3a, by linear functions, as:

$$\varepsilon' = \varepsilon'_0 + \alpha H = \begin{cases} 4 + 0.0148 \cdot H(\text{kA/m}) \\ 35 + 0.18 \cdot H(\text{kA/m}) \\ 1000 + 7.8 \cdot H(\text{kA/m}) \end{cases} \quad (3)$$

where ε'_0 is the relative dielectric permittivity of the hMREs at $H = 0$ and α is a physical quantity that depends on the intensity of the magnetic field and the quantity of the graphene in the hMREs.

Corroborating the results in Figure 3a with Relation (3), it can be observed that in the absence of the magnetic field, the relative dielectric permittivity increases by 8.75 times for the hMRE with $\Phi_{nGr} = 7.15 \text{ wt\%}$ and by 250 times for the hMRE with $\Phi_{nGr} = 14.30 \text{ wt\%}$, compared to the hMRE with $\Phi_{nGr} = 0.00 \text{ wt\%}$. In a magnetic field, the slope of the functions of Figure 3a increase by 12 times for hMRE with $\Phi_{nGr} = 7.15 \text{ wt\%}$ and by 527 times for the hMRE with $\Phi_{nGr} = 14.30 \text{ wt\%}$, compared to the hMRE with no graphene nanoparticle content.

We define the magnitude of the magnetodielectric effect by the expression:

$$MDE(\%) = \frac{\varepsilon' - \varepsilon'_0}{\varepsilon'_0} \cdot 100 \quad (4)$$

where the notations for permittivity are the same as those previously introduced.

In Relation (4), the results of Figure 3a are inserted for the hMREs, and the magnitude of the magnetodielectric effect are obtained in Figure 4.

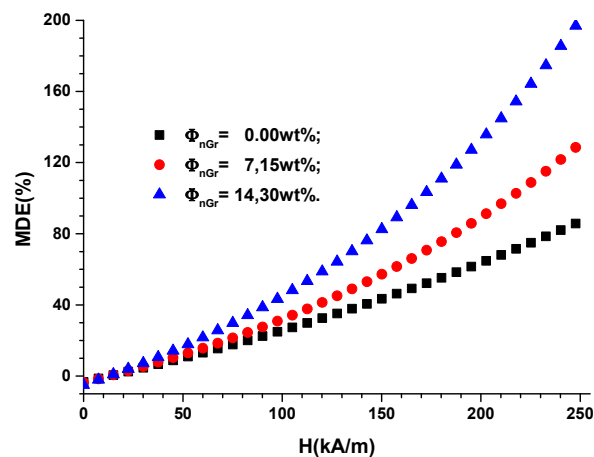


Figure 4. The magnetodielectric effect MDE versus the magnetic field intensity H for the mass fractions Φ_{nGr} of graphene nanoparticles.

The relaxation polarization of silicone rubber [27] coupled with the interfacial one of graphene nanoparticles [30] and the magnetoconstriction phenomenon [6–10] have the effect of increasing MDE with H and Φ_{nGr} , as shown in Figure 4.

Between the electrical conductivity σ and the dielectric loss coefficient D , there is the following relation [28,29]:

$$\sigma = 2\pi f D \quad (5a)$$

where f is the frequency, ε_0 is the dielectric permittivity of the vacuum and D the dielectric loss coefficient.

For the frequency $f = 1000 \text{ Hz}$ the Expression (5a) takes the form

$$10^3 \sigma (\Omega^{-1} m^{-1}) = 6.28 \cdot D \quad (5b)$$

Using Expression (5b) and the the function $D = D(H)_{\Phi_{nGr}}$ from Figure 2b, we obtain the variation of the electrical conductivity $\sigma = \sigma(H)_{\Phi_{nGr}}$ as shown in Figure 3b.

$$10^3 \cdot \sigma = \sigma_0 + \beta \cdot H^2 = \begin{cases} 28 \cdot 10^{-3} + 62 \cdot 10^{-7} H^2 \\ 11 \cdot 10^{-2} + 22 \cdot 10^{-6} H^2 \\ 79 \cdot 10^{-2} + 13 \cdot 10^{-5} H^2 \end{cases} \quad (6)$$

where σ_0 is the electric conductivity of the hMREs in the absence of the magnetic field and β is the quantity that is measured in $\Omega^{-1} \text{m}^{-3} \text{kA}^{-2}$.

Based on Figure 3b and Expression (6), it can be observed that by adding graphene nanoparticles, the electron transfer through the SR increases [27,30], which has the effect of increasing the electric conductivity by 3.92 times for the hMRE with $\Phi_{nGr} = 7.15 \text{ wt\%}$ and 28.21 times for the hMRE with $\Phi_{nGr} = 14.30 \text{ wt\%}$ compared to the hMRE with no graphene nanoparticles.

The parameter β from Expression (6) increased by 3.55 times for the hMRE with $\Phi_{nGr} = 7.15 \text{ wt\%}$ and 20.97 times for the hMRE with $\Phi_{nGr} = 14.30 \text{ wt\%}$ compared to the hMRE with no graphene content. The increase of parameter β in a magnetic field is due to the constriction effect of the hMREs, as reported in Ref. [27]. On the other hand, the increase of β with the mass fraction Φ_{nGr} is due to the facilitation of the electron transport by graphene, as shown in Ref. [30].

3. Materials and Methods

3.1. Materials

The necessary materials for producing hMREs and flat capacitors (FCs) are:

- Silicone Rubber (SR), from RTV-Silicone, a product having a white color, and density 2.30 g/cm^3 ;
- Silicone Oil (SO), type C3518 from Sigma-Aldrich, with density 1.08 g/cm^3 ;
- Carbonyl Iron (CI), type C3518, from Sigma-Aldrich, in the shape of spherical particles having diameters between $4.5 \mu\text{m}$ and $5.4 \mu\text{m}$, a Fe content of at least 97% and a density of 7.86 g/cm^3 ;
- Graphene NanoPowder (nGr), from Sky Spring Nanomaterials Inc., powder with Platelet Nanopowder of thickness between 6 nm and 8 nm, average diameter of $15 \mu\text{m}$ Graphene and density 2.28 g/cm^3 ;
- gauze bandage (FT), from MKD Medicala with a granulation of 30 g/cm^3 ;
- six textolite plates (TCu), copper-plated, from Sierra Modellsport.

3.2. The Manufacturing of the hMRE Membranes

Stage 1: In a beaker, the mixture of SR with CI and nGr is homogenized for about 30 min, in the proportions specified in Table 1. After 30 min, S_1 , S_2 and S_3 samples were obtained, in the form of dark, viscous liquids.

Table 1. Sample compositions.

S_i	SR(g)	SO(g)	CI(g ³)	nGr(g)
S_1	6.90	1.08	7.86	0.00
S_2	5.75	1.08	7.86	1.13
S_3	4.60	1.08	7.86	2.26

Stage 2: The FT, from MKD Medicala (Figure 5a), is reduced to the dimensions of $50 \text{ mm} \times 40 \text{ mm}$. Three packets are prepared from the FT, each having a thickness of 6 mm.

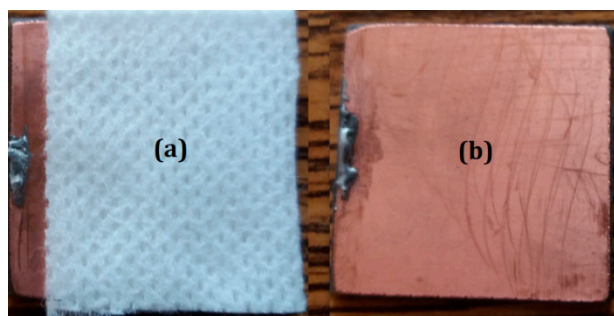


Figure 5. (a) Absorbent fabric (FT); (b) copper-plated plates (TCu).

Stage 3: The first batch is impregnated with sample S_1 the second batch with sample S_2 and finally, the third batch with sample S_3 . Unpolymerized membranes M_1 , M_2 and M_3 are obtained (Table 2).

Table 2. Membrane volume fractions ¹.

M_i	$\Phi_{SR}(\text{wt}\%)$	$\Phi_{SO}(\text{wt}\%)$	$\Phi_{CI}(\text{wt}\%)$	$\Phi_{nGr}(\text{wt}\%)$
M_1	43.60	6.82	49.68	0.00
M_2	36.35	6.82	49.68	7.15
M_3	30.60	6.82	49.68	14.30

¹ $\Phi_{SR}(\text{wt}\%)$, $\Phi_{SO}(\text{wt}\%)$, $\Phi_{CI}(\text{wt}\%)$ and $\Phi_{nGr}(\text{wt}\%)$ are the mass fractions of silicone rubber, silicone oil, carbonyl iron microparticles and graphene nanoparticles.

Stage 4: Using the TCu plates, three packets are made, with two plates in each packet. The TCu plates have a square shape with a side of 50 mm. One by one, the membranes M_1 , M_2 and M_3 are placed between the TCu plates, with the coppered faces towards the membranes. Each packet is pressed until the distance between the plates is 1.2 mm, after which they are left in air. After approximately 24 h, the membranes M_1 , M_2 and M_3 polymerize between the TCu plates. Three flat capacitors are obtained (Figure 6), which are denoted with FCs. The configuration of the obtained membranes is shown in Figure 7.

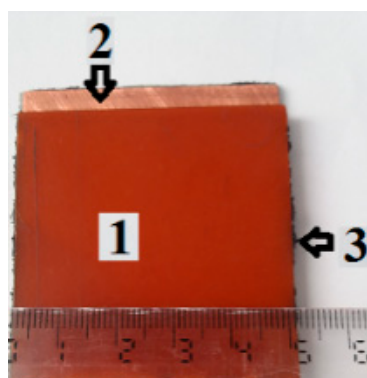


Figure 6. Flat capacitor: 1—TCu plate; 2—copper-plated side of the TCu; 3—hMRE.

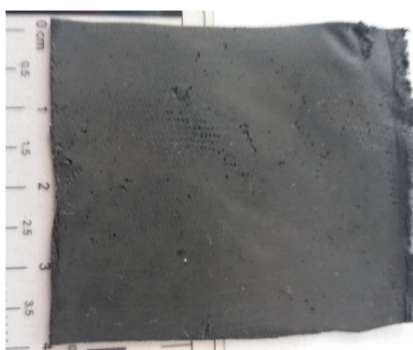


Figure 7. hMRE configuration.

3.3. Experimental Setup

The experimental setup used to study the magnetodielectric effects of the hMRE membranes is that shown in Figure 1 and consists of:

- A—neodymium permanent magnet, type VMM12-N54, generating the magnetic field of intensity H ;
- B—RLC bridge, type ET7-20, from MNIPI (Republic of Belarus);
- Gs—Gaussmeter, Type DX-102;
- FC—working capacitor, fixed on the Hall probe through a spacing device (not represented in Figure 1) that has a micrometre screw;

By turning a screw (not shown in Figure 1), the distance between the permanent magnet and the plane capacitor determines the intensity of the magnetic field.

4. Conclusions

The hybrid magnetorheological elastomers (hMREs) can be successfully manufactured using a mixture of silicone rubber, silicone oil, carbonyl iron microparticles and graphene nanoparticles, absorbed in a cotton fabric. It is shown that the relative dielectric permittivity and electrical conductivity of hMREs increase with an increasing external magnetic field intensity and are significantly influenced by the amount of graphene used. The results obtained are due to the relaxation polarization of the silicone rubber, cumulated with that of the interfacial polarization of the graphene, due to the facilitation of the electron transport by the graphene and due to the magnetoconstriction of the hMREs when a magnetic field is applied.

Author Contributions: Conceptualization, I.B. and O.M.B.; methodology, I.B.; validation, I.B. and O.M.B.; formal analysis, I.B. and O.M.B.; investigation, I.B.; resources, I.B. and O.M.B.; data curation, I.B.; writing—original draft preparation, I.B.; writing—review and editing, O.M.B.; supervision, I.B. and O.M.B.

Funding: This work was supported by a grant of the Romanian National Authority for Scientific Research, CNDI-UEFISCDI, project number PN-III-1.2-PCCDI-2017-0871. Collaboration between JINR and West University of Timisoara is acknowledged.

Conflicts of Interest: The authors declare no conflict of interest

Abbreviations

MRE	Magnetorheological elastomer
hMRE	Hybrid magnetorheological elastomer
FC	Flat capacitor
SR	Silicone rubber
CI	Carbonyl iron
nGr	Graphene nanoparticles
FT	Gauze bandage
TCu	Copper-plated textolite plates

References

1. Rabbani, Y.; Ashtiani, M.; Hashemabadi, S.H. An experimental study on the effects of temperature and magnetic field strength on the magnetorheological fluid stability and MR effect. *Soft Matter* **2015**, *11*, 4453–4460. [[CrossRef](#)] [[PubMed](#)]
2. Lee, S.; Shin, K.Y.; Jang, J. Enhanced magnetorheological performance of highly uniform magnetic carbon nanoparticles. *Nanoscale* **2015**, *7*, 9646–9654. [[CrossRef](#)] [[PubMed](#)]
3. Biller, A.M.; Stolbov, A.V.; Raikher, Y.L. Modeling of particle interactions in magnetorheological elastomers. *J. Appl. Phys.* **2014**, *116*, 114904. [[CrossRef](#)]
4. Sedlacik, M.; Mrilik, M.; Babayan, V.; Pavlinek, V. Magnetorheological elastomers with efficient electromagnetic shielding. *Compos. Struct.* **2016**, *135*, 199–204. [[CrossRef](#)]
5. Jung, H.S.; Kwon, S.H.; Choi, H.J.; Jung, J.H.; Kim, Y.G. Magnetic carbonyl iron/natural rubber composite elastomer and its magnetorheology. *Compos. Struct.* **2016**, *136*, 106–112. [[CrossRef](#)]
6. Bunoiu, M.; Bica, I. Magnetorheological elastomer based on silicone rubber, carbonyl iron and Rochelle salt: Effects of alternating electric and static magnetic fields intensities. *J. Ind. Eng. Chem.* **2016**, *37*, 312–318. [[CrossRef](#)]
7. Balasoiu, M.; Bica, I. Composite magnetorheological elastomers as dielectrics for plane capacitors: Effects of magnetic field intensity. *Results Phys.* **2016**, *6*, 192–202. [[CrossRef](#)]
8. Balasoiu, M.; Lebedev, V.T.; Raikher, Y.L.; Bica, I.; Bunoiu, M. The implicit effect of texturizing field on the elastic properties of magnetic elastomers revealed by SANS. *J. Magn. Magn. Mat.* **2017**, *431*, 126–129. [[CrossRef](#)]
9. Bica, I.; Anitas, E.M.; Bunoiu, M.; Vatzulik, B.; Juganaru, I. Hybrid magnetorheological elastomer: Influence of magnetic field and compression pressure on its electrical conductivity. *J. Ind. Eng. Chem.* **2014**, *20*, 3994–3999. [[CrossRef](#)]
10. Bica, I. Magnetorheological elastomer-based quadrupolar element of electric circuits. *Mat. Sci. Eng. B* **2010**, *166*, 94–98. [[CrossRef](#)]
11. Plachy, T.; Kratina, O.; Sedlacik, M. Porous magnetic materials based on EPDM rubberfilled with carbonyl iron particles. *Compos. Struct.* **2018**, *192*, 126–130. [[CrossRef](#)]
12. Cvek, M.; Kracalik, M.; Sedlacik, M.; Mrilik, M.; Sedlarik, V. Reprocessing of injection-molded magnetorheological elastomers based on TPE matrix. *Compos. Part B* **2019**, *172*, 253–261. [[CrossRef](#)]
13. Moucka, R.; Sedlacik, M.; Cvek, M. Dielectric properties of magnetorheological elastomers with different microstructure. *Appl. Phys. Lett.* **2018**, 122901. [[CrossRef](#)]
14. Ausanio, G.; Iannotti, V.; Ricciardi, E.; Lanotte, L.; Lanotte, L. Magneto-piezoresistance in Magnetorheological elastomers for magnetic induction gradient or position sensors. *Sens. Actuators A* **2014**, *205*, 235–239. [[CrossRef](#)]
15. Li, Y.; Li, J.; Li, W.; Du, H. A state-of-the-art review on magnetorheological elastomer devices. *Smart Mater. Struct.* **2014**, *23*, 123001. [[CrossRef](#)]
16. Sun, S.; Yang, J.; Du, H.; Zhang, S.; Yan, T.; Nakano, M.; Li, W. Development of magnetorheological elastomers-based tuned mass damper for building protection from seismic events. *J. Intell. Mater. Syst. Struct.* **2018**, *29*, 1777–1789. [[CrossRef](#)]
17. Pössinger, T. Experimental Characterization, Modeling and Simulation of Magneto-Rheological Elastomers. Ph.D. Thesis, École Polytechnique Université Paris-Saclay, Palaiseau, France, 2015.
18. Böse, H.; Rabindranath, R.; Ehrlich, J. Soft magnetorheological elastomers as new actuators for valves. *J. Intellig. Mater. Syst. Struct.* **2012**, *23*, 989–994. [[CrossRef](#)]
19. Huang, X.G.; Yan, Z.Y.; Liu, C.; Li, G.H.; Wang, J. Study on the resistance properties of magnetorheological elastomer. *Mater. Res. Innov.* **2015**, *19*, 924–928. [[CrossRef](#)]
20. Wang, Y.; Xuan, S.; Dong, B.; Xu, F.; Gong, X. Stimuli dependent impedance of conductive magnetorheological elastomers. *Smart Mater. Struct.* **2016**, *25*, 025003. [[CrossRef](#)]
21. Bica, I. Electroconductive Magnetorheological Suspensions: Production and Physical Processes. *J. Ind. Eng. Chem.* **2009**, *15*, 233–237. [[CrossRef](#)]
22. Pavlenko, A.V.; Turik, A.V.; Reznichenko, L.A.; Shilkina, L.A.; Konstantinov, G.M. The magnetodielectric effect in $\text{Bi}_{1/2}\text{La}_{1/2}\text{MnO}_3$ ceramics. *Tech. Phys. Lett.* **2013**, *39*, 78–80. [[CrossRef](#)]
23. Fannin, P.C.; Scaife, B.K.; Charles, S.W. On the permittivity of magnetic colloids subject to a strong external magnetic field over the frequency range 50 kHz to 1 MHz. *J. Magn. Magn. Mater.* **1993**, *122*, 168–171. [[CrossRef](#)]

24. Kubisz, L.; Skumiel, A.; Pankowski, E.; Jezierska, D.H. Magnetically induced anisotropy of electric permittivity in the PDMS ferromagnetic gel. *J. Non-Cryst. Solids* **2011**, *357*, 767–770. [[CrossRef](#)]
25. Semisalova, A.S.; Perov, N.S.; Stepanov, G.V.; Kramarenko, E.Y.; Khokhlov, A.R. Strong magnetodielectric effects in magnetorheological elastomers. *Soft Mater* **2013**, *9*, 11318–11324. [[CrossRef](#)]
26. Bica, I.; Anitas, E.M. Magnetodielectric effects in membranes based on magnetorheological bio-suspensions. *Mater. Des.* **2018**, *155*, 317–324. [[CrossRef](#)]
27. Bica, I.; Anitas, E.M. Magnetic field intensity and graphene concentration effects on electrical and rheological properties of MREs-based membranes. *Smart Mater. Struct.* **2017**, *26*, 105038. [[CrossRef](#)]
28. Petrin, A.B. Notes on the Microscopic Theory of Dielectric Polarization. *High Temp.* **2013**, *51*, 147–152. [[CrossRef](#)]
29. Moliton, A. *Applied Electromagnetism and Materials*; Springer: New York, NY, USA, 2007.
30. Li, Y.C.; Li, R.K.Y.; Tjong, S.C. Frequency and Temperature Dependences of Dielectric Dispersion and Electrical Properties of Polyvinylidene Fluoride/Expanded Graphite Composites. *J. Nanomater.* **2010**, *2010*, 261748. [[CrossRef](#)]



© 2019 by the authors. Licensee MDPI, Basel, Switzerland. This article is an open access article distributed under the terms and conditions of the Creative Commons Attribution (CC BY) license (<http://creativecommons.org/licenses/by/4.0/>).